



Lattice thermal conduction in cadmium arsenide

R F Chinnappagoudra, M D Kamatagi, N R Patil, and N S Sankeshwar

Citation :Chin. Phys. B, 2022, 31 (11): 116301. DOI: 10.1088/1674-1056/ac7863

What follows is a list of articles you may be interested in

Tunable anharmonicity *versus* high-performance thermoelectrics and permeation in multilayer $(\text{GaN})_{1-x}(\text{ZnO})_x$

Hanpu Liang(梁汉普) and Yifeng Duan(段益峰)

Chin. Phys. B, 2022, 31 (7): 076301. DOI: 10.1088/1674-1056/ac5c38

Maximum entropy mobility spectrum analysis for the type-I Weyl semimetal TaAs

Wen-Chong Li(李文充), Ling-Xiao Zhao(赵凌霄), Hai-Jun Zhao(赵海军), Gen-Fu Chen(陈根富), and Zhi-Xiang Shi(施智祥)

Chin. Phys. B, 2022, 31 (5): 057103. DOI: 10.1088/1674-1056/ac2b24

Electronic structures of vacancies in $\text{Co}_3\text{Sn}_2\text{S}_2$

Yuxiang Gao(高于翔), Xin Jin(金鑫), Yixuan Gao(高艺璇), Yu-Yang Zhang(张余洋), and Shixuan Du(杜世萱)

Chin. Phys. B, 2021, 30 (7): 077102. DOI: 10.1088/1674-1056/abfa05

Giant topological Hall effect of ferromagnetic kagome metal Fe_3Sn_2

Qi Wang(王琦), Qiangwei Yin(殷蔷薇), Hechang Lei(雷和畅)

Chin. Phys. B, 2020, 29 (1): 017101. DOI: 10.1088/1674-1056/ab5fbc

Thermal transport in semiconductor nanostructures, graphene, and related two-dimensional materials

Alexandr I. Cocemasov, Calina I. Isacova, Denis L. Nika

Chin. Phys. B, 2018, 27 (5): 056301. DOI: 10.1088/1674-1056/27/5/056301

Lattice thermal conduction in cadmium arsenide

R F Chinnappagoudra^{1,2}, M D Kamatagi^{1,†}, N R Patil³, and N S Sankeshwar⁴

¹Department of Physics, S. S. Government First Grade College, Nargund-582 207, Karnataka, India

²Research Resource Centre, Visvesvaraya Technological University, Belagavi-590 018, Karnataka, India

³Department of Physics, B V B College of Engineering and Technology, Hubli, Karnataka 580031, India

⁴Department of Physics & Electronics, CHRIST (Deemed to be University), Bangalore-560 029, Karnataka, India

(Received 1 April 2022; revised manuscript received 8 June 2022; accepted manuscript online 14 June 2022)

Lattice thermal conductivity (LTC) of cadmium arsenide (Cd_3As_2) is studied over a wide temperature range (1–400 K) by employing the Callaway model. The acoustic phonons are considered to be the major carriers of heat and to be scattered by the sample boundaries, disorder, impurities, and other phonons *via* both Umklapp and normal phonon processes. Numerical calculations of LTC of Cd_3As_2 bring out the relative importance of the scattering mechanisms. Our systematic analysis of recent experimental data on thermal conductivity (TC) of Cd_3As_2 samples of different groups, presented in terms of LTC, κ_L , using a nonlinear regression method, reveals good fits to the TC data of the samples considered for $T < \sim 50$ K, and suggests a value of 0.2 for the Gruneisen parameter. It is, however, found that for $T > 100$ K the inclusion of the electronic component of TC, κ_e , incorporating contributions from relevant electron scattering mechanisms, is needed to obtain good agreement with the TC data over the wide temperature range. More detailed investigations of TC of Cd_3As_2 are required to better understand its suitability in thermoelectric and thermal management devices.

Keywords: dirac semimetals, Cd_3As_2 , thermal conductivity, phonon scattering

PACS: 63.20.kp, 63.20.K-, 71.55.Ak, 74.25.F-

DOI: 10.1088/1674-1056/ac7863

1. Introduction

Cadmium arsenide (Cd_3As_2), a 3D II–V material with a tetragonal crystal structure, is a Dirac semimetal with a characteristic linear dispersion ($E = \hbar v_f k$) and is known to possess interesting electronic properties such as high room temperature carrier mobility ($\mu \sim 10^7 \text{ cm}^2 \cdot \text{V}^{-1} \cdot \text{s}^{-1}$), large thermoelectric power ($S \sim 600 \mu\text{V} \cdot \text{K}^{-1}$), high carrier concentration ($n \sim 10^{24} \text{ m}^{-3}$), low resistivity ($\rho \sim 11.6 \text{ n}\Omega \cdot \text{cm}$), and low thermal conductivity ($\kappa \sim 10 \text{ W} \cdot \text{m}^{-1} \cdot \text{K}^{-1}$).^[1–7] Consequently, it has attracted a great deal of attention as a probable candidate for various applications in opto- and magneto-electronic and thermoelectric devices.^[7,8] The interest in Cd_3As_2 as a promising thermoelectric material arises due to not only its attractive electronic properties but also its very-low thermal conductivity. Recently, a larger-than-unity value for the thermoelectric figure of merit, $Z (= S^2/\rho\kappa)$, has been reported for Cd_3As_2 in the presence of a magnetic field.^[9–14] However, to obtain a better understanding and a clear perspective of the suitability of Cd_3As_2 in not only thermoelectric devices but also thermal management issues, it becomes crucial and imperative for a detailed study of the property of thermal conductivity (TC) in this technologically important material.

In the presence of a thermal gradient applied across a semiconducting material sample, the heat energy is carried predominantly by the phonons of the acoustic mode, the contribution from the charge carriers is small. Correspondingly, the thermal conductivity (TC) of the material, κ , is due to two contributions, namely, κ_L from the lattice, and κ_e from

the charge carriers. In general, the TC of a material is known to exhibit a typical temperature dependence: with increase in temperature, the TC at first (for $T < \sim 5$ K) is found to increase as T^3 due to phonon-boundary scattering, then reaches a maximum κ_{max} around $T_{\text{max}} \sim 0.05\Theta_D$ with Θ_D being the Debye temperature, due to phonon–impurity and phonon–phonon scatterings, and finally at higher temperatures decreases as T^{-1} , owing to dominance of phonon–phonon scattering. Further, in the case of degenerate material samples, κ_e can become appreciable at higher temperatures.

In literature, there exist a few investigations on the thermal properties of Cd_3As_2 , and most of them are experimental. Among the first experimental reports on TC of Cd_3As_2 is the study of Spitzer *et al.*^[15] In their measurement of the TC, they reported a very low room-temperature value of $\sim 2.6 \text{ W/m}\cdot\text{K}$ – $2.9 \text{ W/m}\cdot\text{K}$ for undoped samples. Another early investigation on TC was the study by Armitage and Goldsmid^[16] on different samples over the temperature range $T \sim 8 \text{ K}$ – 300 K . They found that, with increasing temperature, the lattice thermal conductivity (LTC) of Cd_3As_2 falls continuously as $\kappa_L \sim T^{-1}$ for $T > \sim 10 \text{ K}$, reaching a value of about $1 \text{ W/m}\cdot\text{K}$ at 300 K , suggesting predominance of phonon–phonon scattering. They have also suggested that a maximum may exist just below 8 K , with imperfection scattering playing a major role at liquid helium temperatures. Combarieu and Jay-Gerin,^[17] in their measurement of the specific heat of Cd_3As_2 at low temperatures ($1.7 \text{ K} < T < \sim 30 \text{ K}$), showed that the specific heat is dominated by the lattice contribution. They found a value of 111 K

[†]Corresponding author. E-mail: indmalleesh@gmail.com

for Θ_D . Bortkowski *et al.*^[18] have reported measurements of TC over the temperature range from 4.2 K to 40 K in Cd_3As_2 samples oriented in different crystallographic directions. They found the TC to depict a well-defined maximum around 6 K and to be characterized by anisotropy. Zhang *et al.*^[11] reported the observation of low TC, one order of magnitude lower than the conventional metals or semimetals with similar electrical conductivity. In their analysis of the temperature-dependent TC of undoped Cd_3As_2 , the significant enhancement in TC observed below 50 K is found to follow a T^{-1} dependence, suggesting that phonon–phonon scattering is the main reason for the low value of TC. Recently, Wang *et al.*^[10] reported measurements of the temperature dependence of TC of four Cd_3As_2 single crystals with different carrier concentrations in the presence of a magnetic field. They found that for their four crystal samples in zero magnetic field, as the temperature increases over a wide temperature range ($10 \text{ K} < T < 500 \text{ K}$), κ first decreases rapidly in the low-temperature range, becomes weakly temperature dependent in the intermediate-temperature range, and then increases in the high-temperature range. Pariari *et al.*^[12] in their study on the effect of magnetic field on validity of the Wiedemann–Franz law, also reported a similar temperature dependence of TC in the Dirac semimetal Cd_3As_2 in zero magnetic field over $20 \text{ K} < T < 350 \text{ K}$. The sharp increase in κ they observed below 50 K also suggests the smaller contribution to the total TC at low temperatures from electronic thermal conductivity (κ_e). Recently, Yue *et al.*^[19] using first principles calculations and temperature-dependent high-resolution Raman spectroscopy, described the ultralow LTC of Cd_3As_2 for $T > 100 \text{ K}$, based on soft-mode-enhanced phonon–phonon scatterings. They ascribed the observed^[10] anomalous temperature dependence of TC around 450 K to an interplay between the phonon–phonon Umklapp scattering rates and the soft optical phonon frequency.

So far, there have been only a few reports^[20–22] with regard to theoretical investigations of thermal transport properties of Cd_3As_2 . Lundgren *et al.*^[21] in their analytical study of the thermoelectric properties of Weyl and Dirac semimetals, used a semiclassical Boltzmann approach to investigate the effect of various electron relaxation processes due to charged impurities, short-range disorder and electron–electron interactions on the electronic contribution to TC. They ignored the κ_L contribution from phonons to the TC. Recently, solving the Boltzmann transport equation using an iteration technique, Amarnath *et al.*^[22] studied the temperature dependence of κ_e considering contributions from various electron scattering mechanisms. Their attempt to explain the TC data of Wang *et al.*^[10] Zhang *et al.*^[11] and Pariari *et al.*^[12] in terms of only the electronic contribution could obtain agreement only for $T > \sim 100 \text{ K}$.

We note here that these studies indicate that the tem-

perature dependence of TC of Cd_3As_2 exhibits a typical behavior.^[10–13] With decrease in temperature from $T \sim 400 \text{ K}$, the TC is found to, at first, show a decreasing trend in the range $400 \text{ K} > T > 200 \text{ K}$, before showing a significant ($\kappa \sim T^{-1}$) increase below $T \sim 50 \text{ K}$, then reach a large value ($\sim 50 \text{ W} \cdot \text{m}^{-1} \cdot \text{K}^{-1}$) near the maximum κ_{max} around $T < \sim 10 \text{ K}$, and finally show a decrease for lower temperatures. It may also be noted that in all the samples of Cd_3As_2 referred to above, the decrease of TC from the boundary scattering is not seen down to $T \sim 5 \text{ K}$, and has been ascribed to the large crystalline size.^[10] Further, there have been theoretical investigations with regard to electronic contribution to TC, and there have not been much attention paid to lattice contribution. In the present work we present a detailed study of LTC of Cd_3As_2 using the Callaway model^[23] over a wide temperature range ($2 \text{ K} < T < 400 \text{ K}$). Further, taking into account the relevant electron and phonon scattering mechanisms, we analyze the available TC data, in terms of both the components, namely, κ_L and κ_e , using a nonlinear regression method, and suggest a value for the Gruniesen parameter. In Section 2, we give the details of the Callaway theory of LTC employed in our study. Our results and discussion are presented in Section 3.

2. Theory

The thermal conductivity of a material, κ , is defined by the relation^[23–26]

$$U = -\kappa \nabla T, \quad (1)$$

where U is the heat flux density in the material produced by the temperature gradient ∇T ; κ , in general, is a tensor. As stated above, the total TC κ is due to two contributions, namely, the LTC, κ_L , and the electronic TC, κ_e :

$$\kappa = \kappa_L + \kappa_e. \quad (2)$$

In literature, different approaches have been used to study the thermal conductivity of materials.^[24–31] In the present work, assuming the heat in the material to be transported mainly by the acoustic phonons, we obtain the expression for the lattice contribution, κ_L , by solving the Boltzmann transport equation for phonons in the relaxation time approximation. The heat transports *via* longitudinal acoustic (LA) and transverse acoustic (TA) phonon modes are quite different and depend on their characteristic frequencies and dispersion.^[29–32] The phonon dispersion of Cd_3As_2 shows that LA and TA modes overlap.^[19] Due to lack of experimental data on the phonon spectrum for this Dirac semimetal, we do not considered here the individual contributions from the LA and TA modes. Assuming the material to be isotropic, we use the Callaway model which uses Debye approximation and considers the av-

erage contribution from the LA and TA modes. In the Callaway model, κ_L can be expressed in the form:^[23–25]

$$\kappa_L = \kappa_1 + \kappa_2, \quad (3)$$

where

$$\kappa_1 = HT^3 \int_0^{\Theta_D/T} dx g(x) \tau^c(x) \quad (4)$$

and

$$\kappa_2 = HT^3 \frac{\left[\int_0^{\Theta_D/T} dx g(x) (\tau^c(x)/\tau^N(x)) \right]^2}{\int_0^{\Theta_D/T} dx g(x) (\tau^c(x)/\tau^N(x)\tau^R(x))}. \quad (5)$$

Here, $g(x) = x^4 e^x / (e^x - 1)^2$, Θ_D is the Debye temperature and $H = k_B^4 / (6\pi^2 v \hbar^3)$, with $v^{-1} = [(1/v_l) + (2/v_t)]/3$ denoting the averaged sound velocity.^[23] In Eq. (5), τ^N denotes the relaxation time for normal (N) phonon processes (N-phonon, N-process) which are non-resistive, and τ^R is the sum of all resistive (R) processes including those due to Umklapp (U) phonons: $(\tau^R)^{-1} = \sum_i (\tau_i)^{-1}$, where τ_i is the phonon relaxation time corresponding to the i^{th} resistive scattering process. The combined relaxation rate $(\tau^c)^{-1}$ is written as $(\tau^c)^{-1} = (\tau^N)^{-1} + (\tau^R)^{-1}$.^[23–26]

2.1. Phonon relaxation times

In the temperature range of interest ($1 \text{ K} < T < 400 \text{ K}$), the flow of heat in a Cd_3As_2 sample is considered to be hindered by the scattering of the phonons, at lower temperatures by the sample boundaries, the various impurities and disorder in it, and at higher temperatures by other phonons, mainly *via* the U-processes.

2.2. Phonon–phonon scattering

The ideal thermal resistance of a material, due to phonon–phonon interactions, arises mainly from the Umklapp three-phonon processes.^[23–26] However, the N-phonons which do not contribute directly to the thermal resistance, are known to influence the other resistive processes.^[30,31] A proper description of the relaxation times for these processes requires a knowledge of the phonon spectrum.^[29–31] In literature, different forms for the phonon–phonon relaxation times have been suggested, based on the crystal symmetry and their dependencies on ω and T .^[30] The phonon–phonon relaxation rates can be expressed as^[29–32]

$$\frac{1}{\tau^N} = B_N \omega^s T^{5-s} \quad (6)$$

and

$$\frac{1}{\tau^U} = B_U \omega^2 T \exp(-\theta_D/3T), \quad (7)$$

where the scattering coefficients B_N and B_U , respectively, characterize the N- and U-phonon–phonon scattering strengths, and are given by^[29–31]

$$B_N = (k_B/\hbar)^{5-s} (\hbar\gamma^2 V_0 / Mv^5), \quad (8)$$

$$B_U = \hbar\gamma^2 / Mv^2 \theta_D. \quad (9)$$

Here, M is the average mass of an atom, $V_0 = a^2 c$ its volume, and γ is the mode averaged Gruneisen parameter.^[30] The value of the exponent s in Eqs. (6) and (8), in the case of N-phonon rates, depends on the crystal symmetry and the phonon mode.^[32]

2.3. Phonon–impurity scattering

The scattering rate for the scattering of phonons by impurities is expressed as^[24–26]

$$(\tau^I)^{-1} = A\omega^4, \quad (10)$$

where $A = V_0\Gamma/4\pi v^3$, with Γ denoting the strength of the scattering from isotopes and point defects, such as substitutional impurities as well as possible strain in a specimen. The value of Γ depends on the concentration of impurities and their mass and radius differences.^[30,31]

2.4. Phonon–disorder scattering

The disorder associated with the imperfections in a solid, such as strain due to impurities, isotopes and dislocations, can also be a source of scattering for phonons. The scattering rate for phonon–disorder interaction is expressed as^[29]

$$(\tau^{D0})^{-1} = D_O \omega^2, \quad (11)$$

where D_O denotes the phonon–disorder scattering strength.

2.5. Phonon–boundary scattering

The scattering of phonons by sample boundaries is assumed to be independent of temperature and frequency, and reads^[30,31]

$$(\tau^B)^{-1} = v/L_E, \quad (12)$$

where L_E represents an effective phonon mean free path of the order of the cross-sectional dimensions of the specimen. It includes effects resulting from sample size, geometry, specular reflection of phonons at the surface, etc., which may lead to deviation from the expected T^3 behavior. L_E can be written in the form^[30]

$$L_E = \left(\frac{1}{L_C} \left(\frac{1-p}{1+p} \right) + \frac{1}{l} \right)^{-1}. \quad (13)$$

For a sample of length l and cross-sectional sides b and t , the Casimir length $L_C = (4bt/\pi)^{1/2}$. The value of the specularity parameter p varies from 0 to 1; whenever $p > 0$, partial specular reflection occurs to decrease the effect of boundary scattering.

3. Results and discussion

We have performed numerical calculations of $\kappa_L(T)$ using Eqs. (3)–(13), for characteristic parameters of Cd_3As_2 :^[17,22,33] $a = 3.189 \text{ \AA}$, $c = 5.185 \text{ \AA}$, $v_L = 3500 \text{ ms}^{-1}$, and $v_T = 2160 \text{ ms}^{-1}$. The Debye temperature depends on the phonon spectrum and is known to be different for the three acoustic modes. However, due to lack of experimental data on phonon spectrum, we take the average value of $\Theta_D = 111 \text{ K}$ reported in Ref. [17]. Unlike the treatment of Asen-Palmer *et al.*,^[31] we do not consider the individual contributions from the LA and TA modes. In the case of N-phonon scattering rates for the bulk tetragonal system, the frequency exponent s in Eqs. (6) and (8) is usually taken as 2 for LA and 1 for TA phonons.^[30,34] However, in literature, other temperature and frequency dependent N-phonon relaxation rates have also been considered to explain experimental data on TC.^[24,34]

With a view to first understand the temperature dependence of the total LTC and the relative importance of the individual contributions due to the various phonon scattering mechanisms limiting LTC in Cd_3As_2 over a wide temperature range, we choose to illustrate the same for parameters characterizing sample A of Wang *et al.*^[10] (see Table 1). It may be mentioned here that, while the boundary scattering coefficient L_E is determined by the sample surface specularly parameter p ($0 < p < 1$), the phonon–phonon scattering coefficients B_N and B_U depend crucially on the material Gruneisen parameter γ . In the absence of clarity on the roles of LA and TA phonons and the frequency dependences of their phonon scattering rates on the thermal conduction processes, we present here calculations of κ_L considering two values for the frequency exponent, namely $s = 1$, often considered typical of TA phonon frequency dependence and $s = 2$, as characteristic of LA phonons. Figure 1 depicts κ_L as a function of temperature, calculated using Eqs. (3)–(13), with $(\tau^R)^{-1} = (\tau^B)^{-1} + (\tau^I)^{-1} + (\tau^{DO})^{-1} + (\tau^U)^{-1}$, for typical values of the scattering parameters: $p = 0.2$, $\Gamma = 1.2 \times 10^{-4}$, $D_0 = 10^{-19} \text{ s}$ and taking $\gamma = 0.2$ and $s = 1$. Curves *a*, *b*, *c* and *d* represent the temperature dependences of the individual contributions due to scattering from sample boundaries, disorder, impurities, and other phonons, respectively. Curve 1 denotes the behavior of the total contribution, κ_L . It is found that each of these scattering mechanisms is operative over certain ranges of temperature. For the values of the parameters chosen, at very low temperatures ($T < 4 \text{ K}$), where phonon-processes are frozen out, κ_L is predominantly determined by boundary and disorder scatterings with characteristic T^3 and T^2 dependences, respectively. With increase in temperature, κ_L reaches a maximum of $\kappa_{\text{max}} \sim 10 \text{ W/mK}$ at $T_{\text{max}} \sim 8 \text{ K}$, where phonon–impurity scattering is found to become important. With further increase in temperature, κ_L is found to decrease as T^{-1} because of phonon–phonon scattering. Our calculations also indicate that the influence of the

phonon–impurity scattering is significant even at higher temperatures ($T > \sim 100 \text{ K}$). The dashed curve in Fig. 1 depicts the temperature dependence of κ_L calculated for the same set of parameters listed above, but with $s = 2$. We notice that in this case, although the variation of κ_L is similar to that calculated with $s = 1$, its magnitude is slightly greater in the range $8 \text{ K} < T < 120 \text{ K}$. With a view to investigate the role of N-phonons in determining LTC, we have also performed calculations of its components, κ_1 and κ_2 , as given by Eqs. (3)–(5), again, for the parameters of sample A of Wang *et al.*^[10] Curves *a* and *b* in the inset in Fig. 1 show, respectively, the temperature dependences of the contributions κ_1 and κ_2 . Curve 1 represents the dependence of the total κ_L . We find that although the contribution from κ_2 , which is due to the N-phonons, is very small for $T < 50 \text{ K}$, it is found to become important at higher temperatures and then tend to saturate κ_L , for $T > 100 \text{ K}$; it is sensitive to the value of Γ .^[31]

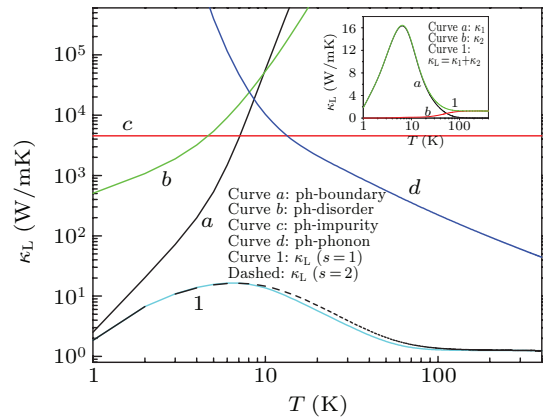


Fig. 1. Temperature dependence of LTC, κ_L , of Cd_3As_2 calculated for the parameters of sample A of Wang *et al.*^[10] Curves *a*, *b*, *c* and *d* depict individual contributions from phonon–boundary, phonon–disorder, phonon–impurity and phonon–phonon scatterings, respectively, to the total κ_L (curve 1), calculated with $s = 1$ in Eq. (6). The dashed line depicts the overall κ_L calculated with $s = 2$. Inset shows the contributions from κ_1 (curve *a*) and κ_2 (curve *b*) to κ_L (curve 1), calculated with $s = 1$.

In the following, we analyze the recent experimental TC data available for six samples of Cd_3As_2 , i.e., four of Wang *et al.*,^[10] one of Zhang *et al.*,^[11] and one of Pariari *et al.*^[12] in terms of LTC, κ_L . In our analysis, we attempt to obtain fits to the data by treating the scattering parameters p , Γ , D_0 and γ as fitting parameters, keeping in view of the relative importance of the various phonon scattering mechanisms determining $\kappa_L(T)$, and noting that, while the parameters p , Γ and D_0 are sample dependent, γ is characteristic of the material. Further, to obtain a good fit with the experimental data for a sample of known dimensions, we vary first the value of p between zero and unity to obtain a fit with the low temperature data, and then that of Γ and D_0 to match the data near the peak value of TC. Using these approximate values of the sample-dependent parameters, we determine the value of the intrinsic high-temperature phonon scattering fitting parameter γ by a nonlinear regression procedure. This is repeated for

each sample. Finally, we systematically finely tune the values of p and Γ to arrive at a single value for γ , the parameter which is characteristic of the material Cd_3As_2 . We find that, with these values of the fitting parameters, p , Γ , D_0 and γ , thus obtained, the value of 0.2 for the average Gruneisen parameter γ describes well the TC data of the six samples considered. We note here that the value of γ , which reflects the strength of the phonon–phonon interactions, needs to be substantiated by experimental studies for Cd_3As_2 . In the case of ZrTe_5 , also a Dirac semimetal, a value of 1.25 is reported from DFT calculations.^[35]

Figures 2(a), 2(b), 2(c) and 2(d), respectively, show the fits we have obtained for the data of samples A, B, C, and D of Wang *et al.*,^[10] which are in the form of single crystals with needle-like shapes. The solid dots, in each of the figures, denote their data obtained for $8\text{ K} < T < 300\text{ K}$. It may be noted that the data for all the samples of Ref. [10] show a variation

of TC typical of the behavior of $\kappa_L(T)$ corresponding to temperatures $T > T_{\text{max}}$: the TC is seen to decrease suddenly for $8\text{ K} < T < \sim 50\text{ K}$ and then to increase slowly for $T > 50\text{ K}$. Curves *a* in Figs. 2(a)–2(d) represent the variation of $\kappa_L(T)$ calculated using Eqs. (3)–(13), with $s = 1$. The values of the fitting parameters used to obtain the fits are listed in Table 1. We notice that our calculations of $\kappa_L(T)$ obtain good fits for all the four samples of Ref. [10], only over the low temperature range, $T < 40\text{ K}$, and that curves *a* underestimate the data for higher temperatures. The dotted line in Fig. 1(a) depicts the variation of $\kappa_L(T)$ calculated with $s = 2$. We further note that the temperature dependence of κ_L calculated with $s = 1$ (curve *a*) is similar to that calculated with $s = 2$ for $T < 50\text{ K}$, and represents the data more closely for higher temperatures. It may however be mentioned that the deviations of $\kappa_L(T)$ from the measured TC noticed in Figs. 1(a)–1(d) for higher temperatures becomes larger with increasing temperatures.

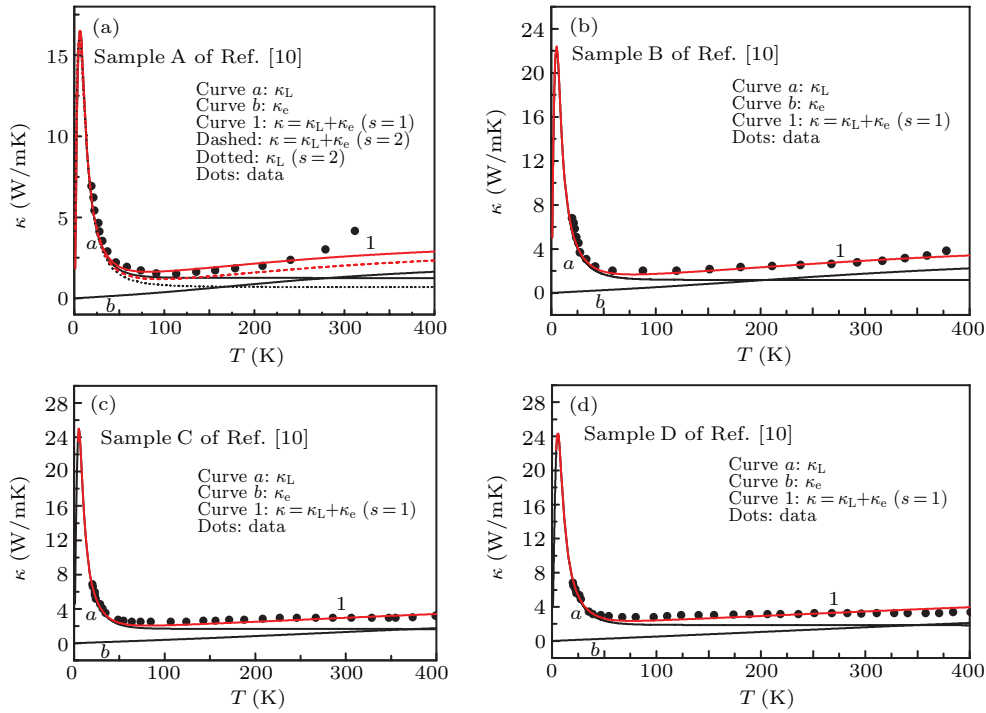


Fig. 2. Temperature dependences of TC of four samples of Cd_3As_2 of Wang *et al.*:^[10] (a) sample A, (b) sample B, (c) sample C, and (d) sample D. Curves *a* and *b*, respectively, represent our calculations of the contributions κ_L and κ_e to the total κ (curve 1), with $s = 1$. Dots denote experimental data. In (a), the dotted and dashed lines, respectively, represent κ_L and κ calculated with $s = 2$.

With a view to obtain a quantitative agreement with the experimental data over the entire range of temperatures, we now examine the contribution of the electronic component $\kappa_e(T)$ to the overall behavior of TC. It may be noted that the electronic TC, κ_e , in semiconductors, though much smaller than the lattice component ($\kappa_e/\kappa_L \sim 0.01$), is expected to become important at higher temperatures, especially in degenerate systems. It is known to display a typical temperature dependence:^[24,25] with increasing temperatures, κ_e , at first increases rapidly, then tends to saturate at higher temperatures; it is very small at very low temperatures and becomes significant at higher temperatures.^[22,24] Here, we employ the Boltz-

mann transport formalism for electrons and express κ_e in the form^[24,25]

$$\kappa_e = \frac{1}{T} \left[K_2 - \frac{K_1^2}{K_0} \right]. \quad (14)$$

With the coefficients K_n given by

$$K_n = \frac{1}{6\pi^2 (\hbar v_F)^3} \int v_k^2 \tau(E_k) (E_k - E_F)^n \times (-\partial f_k^0 / \partial E_k) E_k^2 dE_k. \quad (15)$$

In Eq. (15), $\tau(E_k)$ denotes the overall momentum relaxation time of the electrons with energy E_k and velocity v_k , with other

quantities having their usual meaning.^[20–22] Considering the electrons in Cd₃As₂ to undergo scattering from charged impurities, disorder and acoustic phonons,^[20,21] we have computed the overall electron relaxation rate assuming Matthiessen rule: $(\tau(E_k))^{-1} = \sum_i (\tau_i(E_k))^{-1}$, the explicit expressions for the individual i electron relaxation rates, $(\tau_i(E_k))^{-1}$, being given in Refs. [20,21]. Curves b in Figs. 2(a)–2(d) represent the results of our calculations of κ_e performed using Eq. (14) for characteristic parameters of the Cd₃As₂ samples of Refs. [22,33]: deformation potential constant, $D = 30$ eV, and disorder scattering parameter, $n_d V_0 = 0.16$ (Å⁰)⁻¹. In order to obtain fits to experimental data on TC, κ , at the higher temperatures ($T > 200$ K), we have treated the charged impurity concentration, N_i , as a variable parameter, to alter the magnitude of κ_e . It is observed that, as expected, κ_e is small and shows an increase in magnitude from zero at 0 K to ~ 2 W/mK at 400 K. It is also clear that κ_e can become larger than κ_L at high temperatures ($T > \sim 200$ K). Curves 1 in Figs. 2(a)–2(d) denote the temperature dependences of the total TC, $\kappa = \kappa_L + \kappa_e$, with κ_L calculated with $s = 1$ (curves a). Our calculations are seen to obtain good fits to the data of Ref. [10] for samples B, C and D over the entire range of temperatures (8 K $< T < \sim 400$ K). The values of N_i used for calculating κ_e to obtain the fits are also listed in Table 1. In the case of sample A, the data is found to show a deviation from curve 1 for $T > \sim 300$ K. We have, therefore, performed calculations of $\kappa_L(T)$ for characteristic parameters of sample A, taking $s = 2$. The dashed curve represents the results of our calculations of the total TC, $\kappa = \kappa_L + \kappa_e$, with κ_L calculated with $s = 2$ (dotted curve), and $\kappa_e(T)$ calculated using Eq. (14). However, the dashed curve is found to show a larger deviation from data than that shown by curve 1.

In the case of samples C and D of Wang *et al.*,^[10] we note that the carrier concentrations of these samples are larger than those of samples A and B. Further, their data shows a slow monotonic increase in TC at higher temperatures, suggesting increased electronic contribution to κ . Accordingly, we first attempt to fit the high temperature data ($T > 350$ K) with electronic contribution alone, and then fit the data at lower temperatures following the procedure described above for samples A and B. The parameters used to obtain the fits are listed in Table 1. It may be noted that a good representation of the data is obtained over the entire temperature range. However, a

slight departure from the data is noticed at intermediate temperatures (50 K $< T < 200$ K). This may be ascribed to the lack of sufficient knowledge regarding the phonon dispersion and the consequent simplifications made in our model.

We now present our analysis of the wider-temperature-range (5 K $< T < 375$ K) TC data reported for the other two samples, one of Zhang *et al.*^[11] and the other of Pariari *et al.*^[12] The filled dots in Figs. 3 and 4 represent the data for both the samples. The data show that, with increase in temperature from $T \sim 5$ K, the TC, κ , at first decreases substantially, from a large value, following a T^{-1} dependence mainly due to phonon–phonon scattering till about 50 K–100 K, and then increases slowly, possibly due to the contribution from κ_e .^[10–13] The low-temperature ($T \sim 5$ K) large value of κ is found to be 35 W/m·K for the sample of Ref. [11] and 17 W/m·K for the sample of Ref. [12]. We note here that these two samples possess large electron concentrations in characteristic of degenerate semiconductors (see Table 1). Further, apart from not exhibiting the decrease of κ_L from the boundary scattering for $T < T_{\max}$, they show temperature dependences for typical TC in a semiconductor. In our analysis of their data, we have therefore performed calculations considering contributions from both κ_L and κ_e using Eqs. (3)–(13) and (14), respectively, for characteristic parameters of the samples. Accordingly, we first obtain fits for the high temperature ($T > 350$ K) data with electronic contribution alone, and then follow the procedure described above to obtain the fits to the data at the lower temperatures considering the lattice contribution. In Figs. 3 and 4, curves a represent the variation of the lattice contribution, κ_L , and the curves b represent the electronic contribution, κ_e , for the samples of Zhang *et al.*^[11] and Pariari *et al.*,^[12] respectively. The parameters used to obtain the fits are listed in Table 1. Here, we note that, in the absence of TC peak and sufficient information about the dimensions of the Cd₃As₂ sample of Ref. [12], the value of L_E (instead of p) was varied to match the data near the ‘peak’ value of TC; moreover, the large value of 10 mm obtained for L_E is suggestive of a large phonon mean free path.^[11,12] We find that, with these parameters, very good fits to the data are obtained over the entire temperature range. For instance, our calculations for the sample of Zhang *et al.* show that at 300 K, $\kappa_L = 1.87$ W/mK, which is close to their estimated value of 1.91 W/mK.^[11]

Table 1. Sample parameters and scattering parameters determined from analysis of experimental data on TC of Cd₃As₂ samples of different groups.

| Sample | Dimensions $L \times b \times t$ (mm ³) | Carrier concentration n (10 ²⁴ m ⁻³) | Fitting parameters | | | | |
|----------------|--------------------------------------------------------|------------------------------------------------------------------|--------------------|------------|------------------------------|-----------------------------|-----------------------------------------------------------------------------|
| | | | P | L_E (mm) | Γ (10 ⁻⁴) | D_O (10 ⁻¹⁹ s) | Charged impurity concentration N_i (10 ²³ m ⁻³) |
| A of Ref. [10] | 6.1 × 0.5 × 0.5 | 0.15 | 0.2 | 0.74 | 1.20 | 1.0 | 0.78 |
| B of Ref. [10] | 8.1 × 2.8 × 2.1 | 0.44 | 0.3 | 3.12 | 1.28 | 5.0 | 2.0 |
| C of Ref. [10] | 8.2 × 2.6 × 2 | 1.39 | 0.2 | 2.62 | 0.90 | 8.0 | 12 |
| D of Ref. [10] | 8.4 × 2.5 × 2.2 | 3.30 | 0.15 | 2.51 | 0.8 | 14 | 28 |
| Ref. [11] | – | 10 | – | 10 | 1.2 | 2.0 | 120 |
| Ref. [12] | 3 × 2 × 0.6 | 6.8 | 0.5 | 1.66 | 1.3 | 3.0 | 97 |

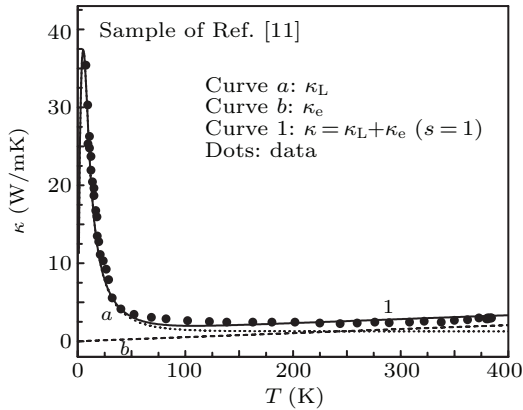


Fig. 3. Variation of TC as a function of temperature for the Cd_3As_2 sample of Zhang *et al.* [11]. Curves *a* (dotted line) and *b* (dashed line), represent our calculations of the lattice and electronic contributions, respectively, to the total TC (curve 1). Dots depict the TC data of the sample in Ref. [11].

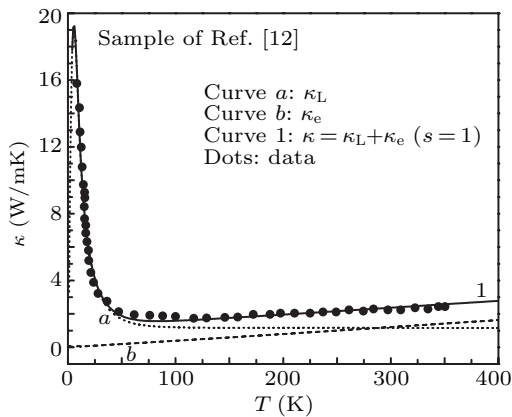


Fig. 4. Temperature variation of TC for the Cd_3As_2 sample of Pariari *et al.* [12]. Curves *a* (dotted line) and *b* (dashed line), respectively, represent lattice and electronic contributions to the total TC (curve 1). Dots depict the TC data of the sample in Ref. [12].

4. Conclusions

We have presented a model for evaluating LTC and analyzed the wide temperature TC data on Cd_3As_2 samples of different research groups using the Callaway model. Good fits with the experimental data are obtained for all the samples considered. A unique value for the Gruneisen parameter characterizing the intrinsic phonon–phonon scattering mechanisms is obtained. The calculations show that, even for high temperatures, LTC is significant. The temperature dependences of both the contributions, LTC and electronic TC, are studied. The present investigation brings out the relative importance of the phonon-scattering mechanisms operative in the Cd_3As_2 system. Recently DFT calculations have reported some details of the phonon spectrum of Cd_3As_2 , suggesting possible contribution from optical phonons. [19,35] A more detailed study of TC of Cd_3As_2 , taking into account the anisotropy of the material and the details of the phonon dispersion and considering the separate contributions from the LA and TA phonon modes as well as from the optical phonons to both the lattice and electronic components of TC, is in progress.

Acknowledgement

This work was supported by University Grants Commission (UGC), India.

References

- [1] Neupane M, Xu S Y, Sankar R, Alidoust N, Bian G, Liu C, Belopolski I, Chang T R, Jeng H T, Lin H, Bansil A, Chou F and Hasan M Z 2014 *Nat. Commun.* **5** 3786
- [2] Liu Z K, Jiang J, Zhou B, Wang Z J, Zhang Y, Weng H M, Prabhakaran D, Mo S K, Peng H, Dudin P, Kim T, Hoesch M, Fang Z, Dai X, Shen Z X, Feng D L, Hussain Z and Chen Y L 2014 *Nat. Mater.* **13** 677
- [3] Liang T, Gibson Q D, Ali M N, Liu M, Cava R J and Ong N P 2015 *Nat. Mater.* **14** 280
- [4] Wang Z, Weng H, Wu Q, Dai X and Fang Z 2013 *Phys. Rev. B* **88** 125427
- [5] Crassee I, Sankar R, Lee W L, Akrap A and Orlita M 2018 *Phys. Rev. Mater.* **2** 120302
- [6] Rosenberg A J and Harman T C 1959 *J. Appl. Phys.* **30** 1621
- [7] Armitage N P, Mele E J and Vishwanath A 2018 *Rev. Mod. Phys.* **90** 015001
- [8] Zhao Y, Liu H, Zhang C, Wang H, Wang J, Lin Z, Xing Y, Lu H, Liu J, Wang Y, Brombosz S M, Xiao Z, Jia S, Xie X C and Wang J 2015 *Phys. Rev. X* **5** 031037
- [9] Zhou T, Zhang C, Zhang H, Xiu F and Yang Z 2016 *Inorg. Chem. Front.* **3** 1637
- [10] Wang H, Luo X, Peng K, Sun Z, Shi M, Ma D, Wang N, Wu T, Ying J, Wang Z and Chen X 2019 *Adv. Funct. Mater.* **29** 1902437
- [11] Zhang C, Zhou T, Liang S, Cao J, Yuan X, Liu Y, Shen Y, Wang Q, Zhao J, Yang Z and Xiu F 2016 *Chin. Phys. B* **25** 017202
- [12] Pariari A, Khan N and Mandal P 2015 arXiv:1502.02264v3 [cond-mat.str-el]
- [13] Pariari A, Khan N, Singha R, Satpati B and Mandal P 2016 *Phys. Rev. B* **94** 165139
- [14] Hosseini T, Yavarishad N, Alward J, Kouklin Z and Gajdardziska-Josifovska M 2016 *Adv. Electron. Mater.* **2** 1500319
- [15] Spitzer D P, Castellion G A and Haacke G 1966 *J. Appl. Phys.* **37** 3795
- [16] Armitage and Goldsmid 1969 *J. Phys. C: Solid State Phys.* **2** 2138
- [17] De Combarieu A and Jay-Gerin J P 1982 *Phys. Rev. B* **25** 2923
- [18] Bartkowski K, Rafalowicz J and Zdanowicz W 1986 *J. Thermophys.* **7** 765
- [19] Yue S, Chorsi H T, Goyal M, Schumann T, Yang R, Xu T, Deng B, Stemmer S, Schuller J A and Liao B 2019 *Phys. Rev. Res.* **1** 033101
- [20] Das Sarma S, Hwang E H and Min H 2015 *Phys. Rev. B* **91** 035201
- [21] Lundgren R, Laurell P and Fiete G A 2014 *Phys. Rev. B* **90** 165115
- [22] Amarnath R, Bhargavi K S and Kubakaddi S S 2020 *J. Phys.: Condens. Matter* **32** 225704
- [23] Callaway J 1959 *Phys. Rev.* **113** 1046
- [24] Berman R 1976 *Thermal Conduction in Solids* (Oxford: Clarendon Press)
- [25] Bhandari C M and Rowe D M 1988 *Thermal Conduction in Semiconductors* (New York: Wiley)
- [26] Klemens P G, in Seitz F and Turnbull D (eds.) 1958 *Solid State Physics* (New York: Academic) Vol. 7 p. 7
- [27] Wan X, Ma D, Pan D, *et al.* 2021 *Mater. Today Phys.* **20** 100445
- [28] Lu L, Ma D, Zhong M and Zhang L 2022 *New J. Phys.* **24** 013007
- [29] Kamatagi M D, Sankeshwar N S and Mulimani B G 2007 *Diamond Rel. Mater.* **16** 98
- [30] Morelli D T, Heremans J P and Slack G A 2002 *Phys. Rev. B* **66** 195304
- [31] Asen-Plamer M, Bartkowski K, Gmelin E, Zhernov A P, Inyushkin A V, Taldenkov A, Ozhogin V I, Itoh K M and Haller E F 1997 *Phys. Rev. B* **56** 9431
- [32] Herring C 1954 *Phys. Rev.* **95** 954
- [33] Kubakaddi S S 2019 *J. Appl. Phys.* **126** 135703
- [34] Jackson H E and Walker C T 1971 *Phys. Rev. B* **3** 1428
- [35] Zhu J, Feng T, Mills S, Wang P, Wu X, Zhang L, Pantelides S T, Du X and Wang X 2018 *ACS Appl. Mater.* **47** 407407